Electronic Supplementary Material (ESI) for RSC Advances.

Supplementary Information

$H_2CO_3 \rightarrow CO_2 + H_2O$ Decomposition in Presence of H_2O, HCOOH, CH_3COOH, H_2SO_4 and HO_2 Radical: Instability of the Gas-Phase H_2CO_3 Molecule in Troposphere and Lower Stratosphere

Sourav Ghoshal and Montu K. Hazra *

Chemical Sciences Division, Saha Institute of Nuclear Physics, 1/AF Bidhannagar,
Kolkata-700 064, India

Table S1: Calculated total electronic energies (E_{total}), zero point vibrational energy (ZPE) corrected total electronic energies [E_{total}(ZPE)] of the monomers, their complexes and transition states (TSs) at the MP2 level in conjunction with the aug-cc-pVDZ, aug-cc-pVTZ and 6-311++G(3df,3pd) basis sets as well as at the CCSD(T)/aug-cc-pVTZ and M062X/aug-cc-pVTZ levels of theories. The values given in the first bracket correspond to the ZPE corrected total electronic energies. The ZPE correction in case of CCSD(T)/aug-cc-pVTZ level of calculations has been done from the MP2/aug-cc-pVTZ level predicted ZPE correction. Imaginary frequencies (ν_{im}) of various transition states (TSs) are given in Table S2.

Monomers/Complexes/ Transition states	**MP2/ aug-cc-pVDZ**	**MP2/ aug-cc-pVTZ**	**MP2/ 6-311++G(3df,3pd)**	**CCSD(T)/ aug-cc-pVTZ**	**M06-2X/ aug-cc-pVTZ**
H_2CO_3	-264.4165077 (-264.377351)	-264.6390758 (-264.599669)	-264.6233828 (-264.583690)	-264.6759153 (-264.6365093)	-265.0237807 (-264.983783)
H_2O	-76.2609098 (-76.239579)	-76.3289923 (-76.307582)	-76.3242865 (-76.302683)	-76.3423255 (-76.3209155)	-76.4300886 (-76.408518)
$(H_2O)_2$	-152.5302069 (-152.484181)	-152.6662408 (-152.620070)	-152.6570272 (-152.610281)	-152.6929627 (-152.6467917)	---
$(H_2O)_3$	-228.8088005 (-228.736294)	-229.012934 (-228.940053)	-228.9989146 (-228.925402)	---	---
CO_2	-188.1697004 (-188.158319)	-188.3216406 (-188.310147)	-188.3119924 (-188.300347)	-188.3405541 (-188.3290601)	-188.5942088 (-188.582240)
HCOOH	-189.3266727 (-189.293000)	-189.4867612 (-189.452905)	-189.4756223 (-189.441573)	-189.5177548 (-189.4838988)	-189.7695724 (-189.735252)
CH_3COOH	-228.5243815 (-228.462658)	-228.7226159 (-228.660459)	-228.7091331 (-228.646761)	-228.7715585 (-228.7094025)	-229.0893386 (-229.027041)
H_2SO_4	-699.0647534 (-699.026747)	-699.4195426 (-699.380442)	-699.4049658 (-699.365152)	-699.4655452 (-699.4264442)	---
HO_2	-150.5685628 (-150.554229)	-150.6926179 (-150.678189)	-150.6800245 (-150.665438)	-150.7262523 (-150.711824)	---

RC-I	-340.6922714 (-340.628613)	-340.9828535 (-340.918805)	-340.9624222 (-340.897887)	-341.0329747 (-340.9689257)	-341.4690169 (-341.404164)
RC-II	-416.9686257 (-416.879637)	-417.3271419 (-417.237794)	-417.3020351 (-417.211915)	-417.3904373 (-417.3010893)	---
RC-III	-416.9727335 (-416.883561)	-417.3314759 (-417.241821)	-417.3062396 (-417.215939)	---	---
RC-IV	-416.9670765 (-416.878641)	-417.325479 (-417.236621)	-417.3002826 (-417.210773)	---	---
RC-V	-493.2496802 (-493.135336)	-493.6763753 (-493.561523)	-493.6464801 (-493.530704)	---	---
RC-VI	-493.2529794 (-493.138692)	-493.6797706 (-493.564890)	-493.6501122 (-493.534241)	---	---
RC-VII	-493.2482299 (-493.134077)	-493.6742485 (-493.559806)	-493.6446102 (-493.529148)	---	---
RC-VIII	-493.2480535 (-493.134073)	-493.6742975 (-493.559911)	-493.6447475 (-493.529319)	---	---
RC-IX	-493.2414344 (-493.127580)	-491.9659088 (-493.553388)	-493.6379932 (-493.522712)	---	---
RC-X	-453.7629031 (-453.687658)	-454.1458869 (-454.070127)	-454.1188934 (-454.042592)	-454.2137177 (-454.1379577)	-454.8128165 (-454.736398)
RC-XI	-492.9619561 (-492.858981	-493.3830236 (-493.279315)	-493.3535843 (-493.249361)	-493.4688795 (-493.3651705)	-494.1338156 (-494.029474)
RC-XII	-963.5009145 (-963.421769)	-964.0788882 (-963.998438)	-964.0490628 (-963.967473)	-964.1617903 (-964.0813403)	---
RC-XIII	-415.0025362 (-414.945816)	-415.3491992 (-415.292058)	-415.3211952 (-415.263491)	-415.419274 (-415.362133)	---

PC-I	-340.7085185 (-340.649244)	-340.9962467 (-340.936707)	-340.9772165 (-340.917050)	-341.0422801 (-340.9827411)	-341.4723743 (-341.411583)
PC-II	-416.9848658 (-416.899863)	-417.3404721 (-417.255151)	-417.3167713 (-417.230709)	-417.3998067 (-417.3144857)	---
PC-III	-416.9783078 (-416.894958)	-417.3339413 (-417.250165)	-417.3101766 (-417.225570)	---	---
PC-IV	-416.9846249 (-416.899656)	-417.3403084 (-417.254988)	-417.3165889 (-417.230508)	---	---
PC-V	-493.2572621 (-493.147609)	-493.6806561 (-493.570696)	-493.6522791 (-493.541307)	---	---
PC-VI	-493.2572621 (-493.147608)	-493.6806561 (-493.570696)	-493.6522791 (-493.541306)	---	---
PC-VII	-493.266396 (-493.155336)	-493.689622 (-493.578314)	-493.6616145 (-493.549151)	---	---
PC-VIII	-493.2653879 (-493.154537)	-493.6889697 (-493.577725)	-493.6610001 (-493.548532)	---	---
PC-IX	-493.2565881 (-493.147150)	-493.6801269 (-493.570270)	-493.6517194 (-493.540859)	---	---
PC-X	-453.7776196 (-453.706708)	-454.1574634 (-454.086258)	-454.1319583 (-454.060081)	-454.2213486 (-454.1501436)	-454.8161089 (-454.743507)
PC-XI	-492.975797 (-492.877084)	-493.3937085 (-493.294454)	-493.3657408 (-493.265851)	-493.4756158 (-493.3763608)	-494.1360752 (-494.035764)
PC-XII	-963.5217515 (-963.446704)	-964 .0916704 (-964.015719)	-964.0632047 (-963.986008)	-964.1706743 (-964.0947233)	---
PC-XIII	-415.0190307 (-414.967000)	-415.3625026 (-415.310231)	-415.3358324 (-415.282954)	-415.4284729 (-415.3762019)	---

TS-I	-340.6534096 (-340.595262)	-340.944682 (-340.885834)	-340.9231985 (-340.864021)	-340.990553 (-340.931705)	-341.4294818 (-341.369928)
TS-II	-416.9351137 (-416.851713)	-417.2948865 (-417.210744)	-417.2691588 (-417.184427)	-417.3540716 (-417.2699296)	---
TS-III	-416.9348773 (-416.851078)	-417.2945312 (-417.209977)	-417.2682978 (-417.183308)	---	---
TS-IV	-416.9317335 (-416.847520)	-417.2902013 (-417.205375)	-417.2640261 (-417.178673)	---	---
TS-V	-493.2173055 (-493.108030)	-493.6455236 (-493.535404)	-493.6149985 (-493.504188)	---	---
TS-VI	-493.2157017 (-493.106991)	-493.6436848 (-493.534069)	-493.6131287 (-493.502729)	---	---
TS-VII	-493.2180714 (-493.107741)	-493.6444557 (-493.533457)	-493.6139118 (-493.501913)	---	---
TS-VIII	-493.2173607 (-493.107245)	-493.6438464 (-493.533068)	-493.6133508 (-493.501626)	---	---
TS-IX	-493.2049799 (-493.096922)	-493.6315157 (-493.522747)	-493.600894 (-493.491297)	---	---
TS-X	-453.7359673 (-453.667803)	-454.1195707 (-454.050616)	-454.0920957 (-454.022720)	-454.1840053 (-454.1150503)	-454.7868646 (-454.716638)
TS-XI	-492.9359857 (-492.839885)	-493.357434 (-493.260359)	-493.3275856 (-493.230155)	-493.440069 (-493.342994)	-494.1083044 (-494.010139)
TS-XII	-963.474115 (-963.402571)	-964.0531083 (-963.980012)	-964.0227964 (-963.948751)	-964.1323593 (-964.0592633)	---
TS-XIII	-414.9813128 (-414.930904)	-415.3279616 (-415.276792)	-415.2994886 (-415.247905)	-415.3885059 (-415.3373359)	---

Table S2: Imaginary frequencies (cm^{-1}) of various transition states for the water monomer (H_2O) assisted reaction pathway (**R-I**), two water molecules assisted reaction pathways (**R-II to R-IV**), three water molecules assisted reaction pathways (**R-V to R-IX**) and formic acid (FA), acetic acid (AA), sulfuric acid (SA) and hydroperoxide (HO_2) radical assisted reaction pathways (**R-X, R-XI, R-XII** and **R-XIII**) at the MP2/aug-cc-pVDZ, MP2/aug-cc-pVTZ, MP2/6-311++G(3df,3pd) and M06-2X/aug-cc-pVTZ levels of calculations.

Transition States	**MP2/ aug-cc-pVDZ**	**MP2/ aug-cc-pVTZ**	**MP2/6-311++G(3df,3pd)**	**M06-2X/ aug-cc-pVTZ**
TS-I (R-I)	-1101.7608	-1094.9682	-1114.7739	-1060.8183
TS-II (R-II)	-587.0721	-589.9679	-586.9436	----
TS-III (R-III)	-1102.9827	-1060.4546	-1081.3382	----
TS-IV (R-IV)	-724.0674	-709.5852	-726.9417	----
TS-V (R-V)	-483.2061	-482.3351	-487.5622	----
TS-VI (R-VI)	-1150.6502	-1105.8685	-1125.2664	----
TS-VII (R-VII)	-519.7970	-489.5446	-466.1246	----
TS-VIII (R-VIII)	-552.1930	-521.1050	-504.9714	----
TS-IX (R-IX)	-833.7140	-861.1048	-877.6139	----
TS-X (R-X)	-1016.8047	-922.9205	-936.7478	-628.8844
TS-XI (R-XI)	-894.7417	-824.4411	-838.8973	-575.6667
TS-XII (R-XII)	-885.8798	-813.8056	-823.6949	----
TS-XIII (R-XIII)	-1226.2370	-1052.9095	-1052.2342	----

Computational methodology, equations and atmospheric concentrations of the water monomer, dimer, FA, AA, SA and HO_2 radical those have been used to estimate of the reaction rates of various pathways as have been discussed in the article:

For the H_2O, $(H_2O)_2$, formic acid (FA), acetic acid (AA), sulphuric acid (SA) and hydroperoxide (HO_2) radical assisted decomposition pathways, as have been discussed in the text and where the isolated H_2CO_3 molecule is directly involved in its decomposition, the decomposition reactions can be written in generalized form in terms of the bimolecular encounters between the H_2CO_3 molecule and X (X ≡ H_2O, $(H_2O)_2$, FA, AA, SA, and HO_2) as:

$$\mathrm{H_2CO_3 + X} \underset{k_{-1}}{\overset{k_1}{\rightleftarrows}} \mathrm{H_2CO_3 \cdots X} \xrightarrow{k_2} \mathrm{CO_2 \cdots H_2O \cdots X} \rightleftarrows \mathrm{CO_2 + H_2O + X} \qquad (1)$$

The above reaction sequence is typically viewed as one involving the formation of the $H_2CO_3\cdots X$ pre-reactive reactant complex (**RC**), which then undergoes unimolecular decomposition via the transition state (**TS**) to form the $CO_2\cdots H_2O\cdots X$ product complex (**PC**) in the exit channel. Applying a steady state approximation to this pre-reactive reactant complex and assuming that it is in equilibrium with the reactants, the reaction rate (ν) for the decomposition of H_2CO_3 in presence of a particular species 'X' can explicitly be written including tunneling correction and reaction degeneracy as:

$$\nu = \sigma * \Gamma * \frac{k_1}{k_{-1}} * k_2 * [\mathrm{H_2CO_3}] * [\mathrm{X}] = \sigma * \Gamma * K_{eq} * k_2 * [\mathrm{H_2CO_3}] * [\mathrm{X}]$$

$$= K_{eq} * k_2' * [\mathrm{H_2CO_3}] * [\mathrm{X}] = k * [\mathrm{H_2CO_3}] * [\mathrm{X}] \qquad (2)$$

Where, $k_2' = \sigma * \Gamma * k_2 \quad \& \quad k = K_{eq} * k_2'$ (3)

In the above equation, the K_{eq} is the equilibrium constant of the pre-reactive complex, k_2 is the rate constant for the unimolecular reaction of the pre-reactive complex leading to the decomposition products, σ is the reaction degeneracy and Γ is the tunneling correction for the reaction. Tunneling corrections are taken into account by assuming unsymmetrical Eckart barrier.[1-4] The values of the equilibrium constant (K_{eq}) for the pre-reactive complex can be calculated according to the equation 4 and the rate constant (k_2) for the unimolecular reaction step involving the pre-reactive complex can be calculated by the conventional transition state theory (TST) according to the equation 5, as given below:[5-8]

$$K_{eq} = \frac{Q_{RC}}{Q_{R_1} * Q_{R_2}} * e^{\frac{-(E_{RC}-E_R)}{RT}} \qquad (4)$$

$$k_2 = \frac{k_b T}{h} * \frac{Q_{TS}}{Q_{RC}} * e^{\frac{-(E_{TS}-E_{RC})}{RT}} \qquad (5)$$

In the above two equations, the various Q denotes the product of electronic, translational, rotational and vibrational canonical partition functions referenced to the zero-point energy of the pre-reactive complex (RC), reactants (R_1 and R_2) and transition state (TS). The k_b and h are respectively the Boltzmann and Planck constants, T is the temperature in Kelvin, and R is the ideal gas constant. Also, the E_{RC}, E_R and E_{TS} denote respectively the ZPE corrected energy of the pre-reactive complex, total energy of the isolated starting reactants (R_1 and R_2) and energy of the transition state. Therefore, according to the above equations, the relative rate between the water monomer and FA assisted decompositions of the H_2CO_3 molecule can be written as:

$$\frac{v_{\mathrm{H_2O}}}{v_{\mathrm{FA}}} = \frac{(K_{eq})_{\mathrm{H_2CO_3\cdots H_2O}}}{(K_{eq})_{\mathrm{H_2CO_3\cdots FA}}} * \frac{(k_2')_{\mathrm{H_2CO_3\cdots H_2O}}}{(k_2')_{\mathrm{H_2CO_3\cdots FA}}} * \frac{[\mathrm{H_2O}]}{[\mathrm{FA}]} \qquad (6)$$

Form the above equation, it is seen that the calculation is very much straightforward if the concentrations of the water and FA, which are basically the catalysts for the decomposition of H_2CO_3 molecule, are known. Thus, one can easily evaluate the relative rates for the decompositions of the H_2CO_3 molecule in presence of the H_2O, $(H_2O)_2$, FA, AA, SA and HO_2 radical; as the concentration of these species in the Earth's atmosphere are known. However, we note that this equation does not work in similar way for other bimolecular reactions those have been considered for the decomposition of the H_2CO_3 molecule in presence of the two and/or three water molecules, in particular, in the pathways where the decompositions of the H_2CO_3 molecules starts from the $H_2CO_3{\cdots}H_2O$ or $H_2CO_3{\cdots}H_2O{\cdots}H_2O$ complexes. This follows as the concentrations of the $H_2CO_3{\cdots}H_2O$ or $H_2CO_3{\cdots}H_2O{\cdots}H_2O$ complexes are also not known. However, these unknown concentrations of the complexes can be expressed by their equilibrium constants and the concentrations of the reactants those form these complexes in terms of bimolecular encounters. For an example, in the case of H_2CO_3 decomposition in presence of the two water molecules with the pathways where second water molecule function either actively or passively to stabilize the pre-reactive $H_2CO_3{\cdots}H_2O$ complex obtained in the water monomer assisted H_2CO_3 decomposition, the decomposition reaction in terms of bimolecular encounters can explicitly be written as:

$$\mathrm{H_2CO_3\cdots H_2O + H_2O \rightleftarrows H_2CO_3\cdots H_2O\cdots H_2O \longrightarrow CO_2\cdots(H_2O)_3 \rightleftarrows CO_2 + 3H_2O} \qquad (7)$$

In the above reaction, the reaction rate for the decomposition of H_2CO_3 molecule via $H_2CO_3{\cdots}H_2O$ complex or the atmospheric loss of the H_2CO_3 molecule depends upon the unknown concentration of the $H_2CO_3{\cdots}H_2O$ complex. However, as mentioned above that the unknown concentration of the $H_2CO_3{\cdots}H_2O$ complex can be expressed by the equilibrium constant for the formation of the $H_2CO_3{\cdots}H_2O$ complex, the relative rate between the single water molecule assisted H_2CO_3 decomposition and the two water molecules assisted H_2CO_3 decomposition according to the pathways of the Reaction-7, as described above, can be written in terms of the equilibrium constant for the formation of the $H_2CO_3{\cdots}H_2O$ complex and the concentrations of the H_2CO_3 and H_2O reactants as:

$$\frac{v_{(\mathrm{H_2O})}}{v_{(\mathrm{2H_2O})}} = \frac{(K_{eq})_{\mathrm{H_2CO_3\cdots H_2O}}}{(K_{eq})_{\mathrm{H_2CO_3\cdots H_2O\cdots H_2O}}} * \frac{(k_2')_{\mathrm{H_2CO_3\cdots H_2O}}}{(k_2')_{\mathrm{H_2CO_3\cdots H_2O\cdots H_2O}}} * \frac{[\mathrm{H_2CO_3}]*[\mathrm{H_2O}]}{[\mathrm{H_2CO_3\cdots H_2O}]*[\mathrm{H_2O}]}$$

$$= \frac{(K_{eq})_{\mathrm{H_2CO_3\cdots H_2O}}}{(K_{eq})_{\mathrm{H_2CO_3\cdots H_2O\cdots H_2O}}} * \frac{(k_2')_{\mathrm{H_2CO_3\cdots H_2O}}}{(k_2')_{\mathrm{H_2CO_3\cdots H_2O\cdots H_2O}}} * \frac{1}{(K_{eq})_{\mathrm{H_2CO_3\cdots H_2O}}} * \frac{1}{[\mathrm{H_2O}]}$$

$$= \frac{1}{(K_{eq})_{\mathrm{H_2CO_3\cdots H_2O\cdots H_2O}}} * \frac{(k_2')_{\mathrm{H_2CO_3\cdots H_2O}}}{(k_2')_{\mathrm{H_2CO_3\cdots H_2O\cdots H_2O}}} * \frac{1}{[\mathrm{H_2O}]} \qquad (8)$$

Therefore, we find from the above equation that the calculation of the relative rate between the water monomer assisted H_2CO_3 decomposition and the two water molecules assisted H_2CO_3 decompositions according to the Reaction 7 is also straightforward if the concentration of the water molecule is known. It is worthwhile to note that the equilibrium constant for the formation of the $H_2CO_3{\cdots}H_2O{\cdots}H_2O$ complex can easily be evaluated by equation 4, as given above. We follow the same approach in case of other various pathways associated with the H_2CO_3 decompositions in presence of the three water molecules. In essence, we note that the relative rates of all the pathways discussed in the article can easily be evaluated if one takes the water monomer and/or water dimer assisted H_2CO_3 decomposition reactions as the references. In Table S3 to S8, we present the overall rate constants ($k = k_2' * K_{eq}$) including the reaction degeneracy and tunneling corrections for all the pathways associated with decompositions of the H_2CO_3 molecule. Note that no tunneling correction has been done for the AA assisted H_2CO_3 decomposition reaction at MP2/aug-cc-pVTZ level of theory, as effective barrier is negative (see text). It is also to be noted here that in our calculations, we have not used any reaction degeneracy (σ) in predicting the equilibrium constants for the formation of $H_2O{\cdots}H_2O$ and $H_2CO_3{\cdots}H_2O$ complexes. However, when we have considered single water molecule as a reactant in the decomposition reactions in terms of bimolecular encounters, the value of $\sigma = 2$ has been used in predicting the overall rate constants.[9]

It has been mentioned in the text that in order to assess the impacts of various decomposition pathways, it is necessary to compare the reaction rates rather than the reaction rate constants. Therefore, given that the rates for all the pathways, discussed above, can be expressed easily with respect to the rate of the water monomer or dimer assisted H_2CO_3 decomposition reaction, we next estimate the concentrations of the water monomer and dimers in the Earth's atmosphere up to 15 km altitude from the Earth's surface (0 km altitude). It is worthwhile to note here that the focus of our work is only to the decompositions of H_2CO_3 molecule in the Earth's troposphere and lower stratosphere. In Table S9, we provide the estimated concentrations of the water monomers and dimers in the 0-15 km altitude range. The concentrations of water dimers have been estimated by following equation 4, as given above. It is seen from the Table S9 that our calculated values for both the water monomers and dimers at different altitudes match well with the values reported in the literature.[10-12] In Table S9, we also provide the concentrations of the FA, AA, SA and HO_2 radical those have been reported in the literature or from the graphical estimates, where the measured values of the concentrations or the mixing ratios are not available directly.[13-31] In case of the FA, we note that two atmospheric profiles are available in terms of the two different ranges of FA concentrations and these two profiles have been reported separately by Razavi[13] and Shephard et al.[14] Importantly, while the atmospheric profile reported by Razavi et al.[13] shows that the mixing ratios of the FA in the altitude range 0 to 15 km are always below 1ppbv, the mixing ratios of the FA in the same altitude range according to the profile reported by Shephard et al.[14] are always above 1ppbv. Therefore, in our relative rate calculations, we take the average values of the FA concentrations according to these two profiles. On the other hand, in case of AA, we don't find atmospheric profiles like those have been reported for the FA. However, we note that the most of the measurements of AA mixing ratios have been reported for the Earth's surface and for lower altitudes of the Earth's atmosphere.[16,19-26] In most of the cases, we find that the mixing ratios of the FA and AA are similar and in other some cases, the mixing ratios of the AA are little bit higher than the mixing ratios of the FA.[19-26] Therefore, to compare the FA and AA assisted H_2CO_3 decompositions on equal footing; the concentrations for both the FA and AA have been taken same in the 0-15 km altitude range. Indeed, and in particular, we note that the reported value for the average AA mixing ratio[15] at 0 km altitude is ~3.8 ppbv and this value matches with the average value (~3.56 ppbv) that we have obtained from the two atmospheric profiles, as mentioned above. It is also worthwhile to note here that this average concentration of the FA or AA at 0 km altitude, which we have taken into account in our rate calculations, is approximately and at least 4 to 5 times higher than the measured concentrations of the FA or AA present in the clean environment of the Earth's atmosphere (see text).

Table S3: Equilibrium constants (K_{eq}) for the formation of pre-reactive complexes, rate constants (k_2) of the unimolecular reactions, tunnelling corrections (Γ) and overall rate constants (k) at the MP2/aug-cc-pVTZ level of calculations for the decompositions of H_2CO_3 in presence of the water monomer and dimer. The units of K_{eq}, k_2 and k are respectively cm^3/molecule, sec^{-1} and (cm^3/molecule) sec^{-1}. The decompositions of H_2CO_3 molecule in presence of the water monomer and dimer have been labelled as **R-I** and **R-II**, as mentioned in the text. The values given in the parenthesis correspond to the results predicted at the CCSD(T)/aug-cc-pVTZ level of calculations.

Altitude (km)	**T (K)**	K_{eq}	k_2	Γ	$k_2'=\sigma*\Gamma*k_2$	$k = K_{eq}*k_2'$
R-I:		$H_2CO_3 + H_2O \rightleftharpoons \underset{\textbf{(RC-I)}}{H_2CO_3\cdots H_2O} \longrightarrow \underset{\textbf{(PC-I)}}{CO_2\cdots(H_2O)_2} \rightleftharpoons CO_2 + 2H_2O$				
0	298.15	9.02×10^{-21}	4.39×10^{-4}	4.21	3.68×10^{-3}	3.31×10^{-23}
		(8.35×10^{-21})	(4.85×10^{-6})	(4.33)	(4.20×10^{-5})	(3.50×10^{-25})
5	259.3	5.54×10^{-20}	2.52×10^{-6}	7.95	4.00×10^{-5}	2.22×10^{-24}
		(5.19×10^{-20})	(1.41×10^{-8})	(8.51)	(2.39×10^{-7})	(1.24×10^{-26})
10	229.7	3.28×10^{-19}	1.72×10^{-8}	18.9	6.50×10^{-7}	2.13×10^{-25}
		(3.05×10^{-19})	(5.02×10^{-11})	(22.25)	(2.23×10^{-9})	(6.80×10^{-28})
15	212.6	1.18×10^{-18}	4.88×10^{-10}	42.37	4.14×10^{-8}	4.88×10^{-26}
		(1.09×10^{-18})	(8.93×10^{-13})	(55.65)	(9.94×10^{-11})	(1.08×10^{-28})
R-II:		$H_2CO_3 + (H_2O)_2 \rightleftharpoons \underset{\textbf{(RC-II)}}{H_2CO_3\cdots(H_2O)_2} \longrightarrow \underset{\textbf{(PC-II)}}{CO_2\cdots(H_2O)_3} \rightleftharpoons CO_2 + 3H_2O$				
0	298.15	8.21×10^{-20}	1.68×10^{-1}	1.44	2.42×10^{-1}	1.99×10^{-20}
		(6.19×10^{-20})	(2.15×10^{-3})	(1.44)	(3.10×10^{-3})	(1.92×10^{-22})
5	259.3	1.53×10^{-18}	2.57×10^{-3}	1.62	4.16×10^{-3}	6.37×10^{-21}
		(1.11×10^{-18})	(1.71×10^{-5})	(1.63)	(2.79×10^{-5})	(3.09×10^{-23})
10	229.7	2.61×10^{-17}	4.47×10^{-5}	1.87	8.36×10^{-5}	2.18×10^{-21}
		(1.81×10^{-17})	(1.58×10^{-7})	(1.89)	(2.99×10^{-7})	(5.41×10^{-24})
15	212.6	1.98×10^{-16}	2.46×10^{-6}	2.09	5.14×10^{-6}	1.02×10^{-21}
		(1.34×10^{-16})	(5.52×10^{-9})	(2.12)	(1.17×10^{-8})	(1.57×10^{-24})

Table S4: Equilibrium constants (K_{eq}) for the formation of pre-reactive complexes, rate constants (k_2) of the unimolecular reactions, tunnelling corrections (Γ) and overall rate constants (k) at the MP2/aug-cc-pVTZ level of calculations for the decompositions of H_2CO_3 in presence of the two water molecules those are associated with the **RC-II**, **RC-III** and **RC-IV** and reaction pathways respectively **R-IIa**, **R-III** and **R-IV**. The reaction path: **R-IIa** is corresponding to the path where the two water molecules actively assist the H_2CO_3 decomposition by a common pre-reactive complex **(RC-II).** The units of K_{eq}, k_2 and k are respectively cm^3/molecule, sec^{-1} and (cm^3/molecule) sec^{-1}.

Altitude (Km)	**T(K)**	K_{eq}	k_2	Γ	$k_2' = \sigma * \Gamma * k_2$	$k = K_{eq} * k_2'$
R-IIa:	$\underset{\textbf{(RC-I)}}{H_2CO_3{\cdots}H_2O} + H_2O \rightleftharpoons \underset{\textbf{(RC-II)}}{H_2CO_3{\cdots}(H_2O)_2} \longrightarrow \underset{\textbf{(PC-II)}}{CO_2{\cdots}(H_2O)_3} \rightleftharpoons CO_2 + 3H_2O$					
0	298.15	5.43×10^{-21}	1.68×10^{-1}	1.44	4.84×10^{-1}	2.63×10^{-21}
5	259.3	3.56×10^{-20}	2.57×10^{-3}	1.64	8.43×10^{-3}	3.00×10^{-22}
10	229.7	2.22×10^{-19}	4.47×10^{-5}	1.89	1.69×10^{-4}	3.75×10^{-23}
15	212.6	8.24×10^{-19}	2.46×10^{-6}	2.13	1.05×10^{-5}	8.64×10^{-24}
R-III:	$\underset{\textbf{(RC-I)}}{H_2CO_3{\cdots}H_2O} + H_2O \rightleftharpoons \underset{\textbf{(RC-III)}}{(H_2CO_3{\cdots}H_2O){\cdots}H_2O} \longrightarrow \underset{\textbf{(PC-III)}}{CO_2{\cdots}(H_2O)_3} \rightleftharpoons CO_2 + 3H_2O$					
0	298.15	1.51×10^{-19}	1.52×10^{-3}	3.64	1.11×10^{-2}	1.76×10^{-21}
5	259.3	1.90×10^{-18}	1.05×10^{-5}	6.09	1.28×10^{-4}	2.43×10^{-22}
10	229.7	2.23×10^{-17}	8.59×10^{-8}	11.87	2.04×10^{-6}	4.55×10^{-23}
15	212.6	1.29×10^{-16}	2.76×10^{-9}	21.31	1.18×10^{-7}	1.52×10^{-23}
R-IV:	$\underset{\textbf{(RC-I)}}{H_2CO_3{\cdots}H_2O} + H_2O \rightleftharpoons \underset{\textbf{(RC-IV)}}{(H_2CO_3{\cdots}H_2O){\cdots}H_2O} \longrightarrow \underset{\textbf{(PC-IV)}}{CO_2{\cdots}(H_2O)_3} \rightleftharpoons CO_2 + 3H_2O$					
0	298.15	6.04×10^{-21}	1.02×10^{-3}	1.72	3.51×10^{-3}	2.25×10^{-23}
5	259.3	3.07×10^{-20}	7.42×10^{-6}	2.09	3.10×10^{-5}	9.52×10^{-25}
10	229.7	1.51×10^{-19}	6.39×10^{-8}	2.64	3.37×10^{-7}	5.09×10^{-26}
15	212.6	4.76×10^{-19}	2.15×10^{-9}	3.22	1.38×10^{-8}	6.59×10^{-27}

Table S5: Equilibrium constants (K_{eq}) for the formation of pre-reactive complexes, rate constants (k_2) of the unimolecular reactions, tunnelling corrections (Γ) and overall rate constants (k) at the MP2/aug-cc-pVTZ level of calculations for the decompositions of H_2CO_3 in the form of $H_2CO_3{\cdots}(H_2O)_2$ + H_2O bimolecular reactants that results in **RC-V** associated with the reaction pathway: **R-V**. The units of K_{eq}, k_2 and k are respectively cm^3/molecule, sec^{-1} and (cm^3/molecule) sec^{-1}.

Altitude (Km)	**T(K)**	K_{eq}	k_2	Γ	$k_2' = \sigma * \Gamma * k_2$	$k = K_{eq} * k_2'$
R-V:	$H_2CO_3{\cdots}(H_2O)_2 + H_2O \rightleftharpoons (H_2CO_3{\cdots}(H_2O)_2){\cdots}H_2O \longrightarrow CO_2{\cdots}(H_2O)_3{\cdots}H_2O \rightleftharpoons CO_2 + 4H_2O$					
	(RC-II)		**(RC-V)**		**(PC-V)**	
0	298.15	3.62×10^{-19}	3.57×10^{-1}	1.28	9.14×10^{-1}	3.31×10^{-19}
5	259.3	5.06×10^{-18}	6.54×10^{-3}	1.38	1.81×10^{-2}	9.13×10^{-20}
10	229.7	6.54×10^{-17}	1.34×10^{-4}	1.52	4.07×10^{-4}	2.66×10^{-20}
15	212.6	4.08×10^{-16}	8.29×10^{-6}	1.63	2.70×10^{-5}	1.10×10^{-20}

Table S6: Equilibrium constants (K_{eq}) for the formation of pre-reactive complexes, rate constants (k_2) of the unimolecular reactions, tunnelling corrections (Γ) and overall rate constants (k) at the MP2/aug-cc-pVTZ level of calculations for the decompositions of H_2CO_3 in the form of $H_2CO_3{\cdots}H_2O$ + $H_2O{\cdots}H_2O$ bimolecular reactants those result in **RC-VI, RC-VII** and **RC-VIII** associated with the reaction pathways respectively: **R-VI, R-VII** and **R-VIII**. The units of K_{eq}, k_2 and k are respectively cm^3/molecule, sec^{-1} and (cm^3/molecule) sec^{-1}.

Altitude (Km)	**T(K)**	K_{eq}	k_2	Γ	$k_2' = \sigma * \Gamma * k_2$	$k = K_{eq} * k_2'$
R-VI:	$H_2CO_3{\cdots}H_2O + (H_2O)_2 \rightleftharpoons (H_2CO_3{\cdots}H_2O){\cdots}(H_2O)_2 \longrightarrow CO_2{\cdots}(H_2O)_3{\cdots}H_2O \rightleftharpoons CO_2 + 4H_2O$					
	(RC-I)		**(RC-VI)**		**(PC-VI)**	
0	298.15	8.27×10^{-17}	5.37×10^{-3}	3.22	1.73×10^{-2}	1.43×10^{-18}
5	259.3	5.99×10^{-15}	4.39×10^{-5}	4.49	1.97×10^{-4}	1.18×10^{-18}
10	229.7	3.74×10^{-13}	4.19×10^{-7}	6.46	2.71×10^{-6}	1.01×10^{-18}
15	212.6	7.12×10^{-12}	1.50×10^{-8}	8.54	1.28×10^{-7}	9.12×10^{-19}
R-VII:	$H_2CO_3{\cdots}H_2O + (H_2O)_2 \rightleftharpoons (H_2CO_3{\cdots}H_2O){\cdots}(H_2O)_2 \longrightarrow CO_2{\cdots}(H_2O)_4 \rightleftharpoons CO_2 + 4H_2O$					
	(RC-I)		**(RC-VII)**		**(PC-VII)**	
0	298.15	6.17×10^{-19}	4.45×10^{-1}	1.30	5.79×10^{-1}	3.57×10^{-19}
5	259.3	1.92×10^{-17}	7.26×10^{-3}	1.41	1.02×10^{-2}	1.97×10^{-19}
10	229.7	5.32×10^{-16}	1.35×10^{-4}	1.54	2.08×10^{-4}	1.11×10^{-19}
15	212.6	5.69×10^{-15}	7.86×10^{-6}	1.66	1.30×10^{-5}	7.42×10^{-20}
R-VIII:	$H_2CO_3{\cdots}H_2O + (H_2O)_2 \rightleftharpoons (H_2CO_3{\cdots}H_2O){\cdots}(H_2O)_2 \longrightarrow CO_2{\cdots}(H_2O)_4 \rightleftharpoons CO_2 + 4H_2O$					
	(RC-I)		**(RC-VIII)**		**(PC-VIII)**	
0	298.15	2.69×10^{-18}	8.61×10^{-2}	1.34	1.15×10^{-1}	3.10×10^{-19}
5	259.3	8.51×10^{-17}	1.28×10^{-3}	1.47	1.88×10^{-3}	1.60×10^{-19}
10	229.7	2.39×10^{-15}	2.20×10^{-5}	1.63	3.59×10^{-5}	8.57×10^{-20}
15	212.6	2.58×10^{-14}	1.21×10^{-6}	1.77	2.14×10^{-6}	5.53×10^{-20}

Table S7: Equilibrium constants (K_{eq}) for the formation of pre-reactive complexes, rate constants (k_2) of the unimolecular reactions, tunnelling corrections (Γ) and overall rate constants (k) at the MP2/aug-cc-pVTZ level of calculations for the decompositions of H_2CO_3 in presence of the formic acid (FA) and acetic acid (AA). The units of K_{eq}, k_2 and k are respectively cm^3/molecule, sec^{-1} and (cm^3/molecule) sec^{-1}. The decompositions of H_2CO_3 molecule in presence of the FA and AA have been labelled as **R-X** and **R-XI**, as mentioned in the text. The values given in the parenthesis correspond to the results predicted at the CCSD(T)/aug-cc-pVTZ level of calculations.

R-X:

$$H_2CO_3 + HCOOH \rightleftharpoons \underset{\textbf{(RC-X)}}{H_2CO_3\cdots HCOOH} \rightarrow \underset{\textbf{(PC-X)}}{CO_2\cdots H_2O\cdots HCOOH} \rightleftharpoons CO_2 + H_2O + HCOOH$$

Altitude (km)	**T (K)**	K_{eq}	k_2	Γ	$k_2'=\sigma*\Gamma*k_2$	$k = K_{eq}*k_2'$
0	298.15	1.68×10^{-19}	1.02×10^{3}	1.76	1.80×10^{3}	3.02×10^{-16}
		(1.67×10^{-19})	(2.78×10^{1})	(2.27)	(6.31×10^{1})	(1.05×10^{-17})
5	259.3	2.45×10^{-18}	4.53×10^{1}	2.04	9.24×10^{1}	2.26×10^{-16}
		(2.44×10^{-18})	(7.18×10^{-1})	(2.95)	(2.12)	(5.17×10^{-18})
10	229.7	3.36×10^{-17}	2.250	2.40	5.40	1.81×10^{-16}
		(3.34×10^{-17})	(2.12×10^{-2})	(3.98)	(8.44×10^{-2})	(2.82×10^{-18})
15	212.6	2.20×10^{-16}	2.65×10^{-1}	2.72	7.21×10^{-1}	1.59×10^{-16}
		(2.19×10^{-16})	(1.72×10^{-3})	(5.04)	(8.67×10^{-3})	(1.90×10^{-18})

R-XI:

$$H_2CO_3 + CH_3COOH \rightleftharpoons \underset{\textbf{(RC-XI)}}{H_2CO_3\cdots CH_3COOH} \rightarrow \underset{\textbf{(PC-XI)}}{CO_2\cdots H_2O\cdots CH_3COOH} \rightleftharpoons CO_2 + H_2O + CH_3COOH$$

Altitude (km)	**T (K)**	K_{eq}	k_2	Γ	$k_2'=\sigma*\Gamma*k_2$	$k = K_{eq}*k_2'$
0	298.15	8.21×10^{-19}	2.81×10^{3}	---	2.81×10^{3}	2.31×10^{-15}
		(7.97×10^{-19})	(9.24×10^{1})	(1.79)	(1.65×10^{2})	(1.32×10^{-16})
5	259.3	1.50×10^{-17}	1.33×10^{2}	---	1.33×10^{2}	2.0×10^{-15}
		(1.32×10^{-17})	(2.89)	(2.13)	(6.16)	(8.13×10^{-17})
10	229.7	2.52×10^{-16}	7.02	---	7.02	1.77×10^{-15}
		(2.43×10^{-16})	(8.42×10^{-2})	(2.56)	(2.16×10^{-1})	(5.24×10^{-17})
15	212.6	1.92×10^{-15}	8.65×10^{-1}	---	8.65×10^{-1}	1.66×10^{-15}
		(1.84×10^{-15})	(7.28×10^{-3})	(2.93)	(2.13×10^{-2})	(3.92×10^{-17})

Table S8: Equilibrium constants (*K_{eq}*) for the formation of pre-reactive complexes, rate constants (*k_2*) of the unimolecular reactions, tunnelling corrections (*Γ*) and overall rate constants (*k*) at the MP2/aug-cc-pVTZ level of calculations for the decompositions of H_2CO_3 in presence of the sulfuric acid (SA) and hydroperoxide (HO_2) radical. The units of *K_{eq}*, *k_2* and *k* are respectively cm^3/molecule, sec^{-1} and (cm^3/molecule) sec^{-1}. The decompositions of H_2CO_3 molecule in presence of SA and HO_2 radical have been labelled as **R-XII** and **R-XIII**, as mentioned in the text. The values given in the parenthesis correspond to the results predicted at the CCSD(T)/aug-cc-pVTZ level of calculations.

Altitude (km)	**T (K)**	**K_{eq}**	**k_2**	**Γ**	**$k_2'=\sigma*\Gamma*k_2$**	**$k = K_{eq}*k_2'$**
R-XII:	$H_2CO_3 + H_2SO_4 \rightleftharpoons H_2CO_3\cdots H_2SO_4 \rightarrow CO_2\cdots H_2O\cdots H_2SO_4 \rightleftharpoons CO_2 + H_2O + H_2SO_4$					
			(RC-XII)	**(PC-XII)**		
0	298.15	3.91×10^{-19}	5.56×10^{3}	0.72	4.00×10^{3}	1.57×10^{-15}
		(4.17×10^{-19})	(1.16×10^{2})	(1.83)	(2.1×10^{2})	(8.85×10^{-17})
5	259.3	6.24×10^{-18}	2.75×10^{2}	0.71	1.95×10^{2}	1.22×10^{-15}
		(6.18×10^{-18})	(3.5)	(2.19)	(7.66)	(4.73×10^{-17})
10	229.7	9.27×10^{-17}	1.52×10^{1}	0.69	1.05×10^{1}	9.72×10^{-16}
		(1.0×10^{-16})	(1.0×10^{-1})	(2.69)	(0.3)	(3.0×10^{-17})
15	212.6	6.44×10^{-16}	1.94	0.69	1.34	8.62×10^{-16}
		(7.04×10^{-16})	(8.61×10^{-3})	(3.15)	(0.03)	(2.1×10^{-17})
R-XIII:	$H_2CO_3 + HO_2 \rightleftharpoons H_2CO_3\cdots HO_2 \rightarrow CO_2\cdots H_2O\cdots HO_2 \rightleftharpoons CO_2 + H_2O + HO_2$					
			(RC-XIII)	**(PC-XIII)**		
0	298.15	8.06×10^{-21}	1.68×10^{5}	1.46	2.45×10^{5}	1.97×10^{-15}
		(5.27×10^{-21})	(6.88)	(3.29)	(2.26×10^{1})	(1.19×10^{-19})
5	259.3	7.51×10^{-20}	1.42×10^{4}	1.61	2.29×10^{4}	1.72×10^{-15}
		(4.61×10^{-20})	(1.27×10^{-1})	(5.14)	(6.53×10^{-1})	(3.01×10^{-20})
10	229.7	6.64×10^{-19}	1.32×10^{3}	1.78	2.35×10^{3}	1.56×10^{-15}
		(3.83×10^{-19})	(2.72×10^{-3})	(8.89)	(2.42×10^{-2})	(9.27×10^{-21})
15	212.6	3.17×10^{-18}	2.43×10^{2}	1.93	4.69×10^{2}	1.49×10^{-15}
		(1.75×10^{-18})	(1.76×10^{-4})	(14.07)	(2.48×10^{-3})	(4.34×10^{-21})

Table S9: Concentrations (molecules/cm^3) of the water monomer (H_2O), dimer [$(H_2O)_2$], formic acid (FA), acetic acid (AA), sulfuric acid (SA) and hydroperoxide (HO_2) radical at different altitude of the Earth's atmosphere. For the calculations of water monomer concentrations in the 0 to 15 km altitude of the Earth's atmosphere, the temperatures (T), pressures (P), air density and mixing ratios (M.R) of water monomers have been taken from ref. 12. The concentrations of water dimers at different altitudes have been estimated by the use of equation 4, as given above, based on the MP2/aug-cc-pVTZ level predicted energies and anharmonic frequencies. In the calculation of the relative reaction rates, the average values of FA and AA concentrations have taken into account and same concentrations have been used, as has been mentioned above.

Altitude (km)	**T (K)**	**P (atm)**	**Air Density**	**(M.R) Ref. 12**	**[H_2O]**	**[$(H_2O)_2$]**	**[FA]**			**[AA]**	**[SA]** [a] **Ref 27**	**[HO_2] Ref 30-31**
							Ref. 13	**Ref. 14**	**Average**			
0	298.15	1	2.5×10^{19}	1.4×10^{-2}	5.54×10^{17}	4.55×10^{14}	1.9×10^{10}	1.6×10^{11}	8.9×10^{10}	8.9×10^{10}	3.7×10^{8}	1.4×10^{8}
5	259.3	0.535	1.5×10^{19}	1.0×10^{-3}	2.43×10^{16}	1.89×10^{12}	3.4×10^{9}	3.7×10^{10}	2.0×10^{10}	2.0×10^{10}	6.0×10^{7}	4.9×10^{7}
10	229.7	0.266	8.5×10^{18}	3.6×10^{-5}	4.92×10^{14}	1.70×10^{9}	5.1×10^{8}	1.6×10^{10}	8.3×10^{9}	8.3×10^{9}	8.3×10^{6}	6.0×10^{7}
15	212.6	0.120	4.2×10^{18}	2.9×10^{-6}	1.96×10^{13}	4.82×10^{6}	8.4×10^{7}	6.3×10^{9}	3.2×10^{9}	3.2×10^{9}	2.4×10^{5}	9.0×10^{6}

[a] Although that the concentration of sulfuric acid (SA) at the Earth's surface according to graphical estimate from the reference 27 is ~3.7×10^{8} molecules per cm^3, the average value of the measured concentration of SA is usually expected to be around one order of magnitude less (see Reference 10, 34-40)

Table S10: Equilibrium constants (K_{eq}) for the formation of pre-reactive complexes, rate constants (k_2) of the unimolecular reactions, tunnelling corrections (Γ) and overall rate constants (k) at the MP2/aug-cc-pVTZ level of calculations for the H_2CO_3 decompositions via the reaction pathways: **R-I**, **R-II**, **R-X**, **R-XI**, **R-XII** and **R-XIII**, as described in the text. The units of K_{eq}, k_2 and k are respectively cm^3/molecule, sec^{-1} and (cm^3/molecule) sec^{-1}. The values given in the parenthesis correspond to the results predicted at the CCSD(T)/aug-cc-pVTZ level of calculations.

Altitude = 0 km, Temperature=320 K

Reaction Pathways	Concentrations	K_{eq}	k_2	Γ	$k_2'=\sigma*\Gamma*k_2$	$k = K_{eq}* k_2'$
R-I	$[H_2O]$	3.99×10^{-21}	4.59×10^{-3}	3.35	3.07×10^{-2}	1.23×10^{-22}
	2.36×10^{18}	(3.78×10^{-21})	(6.92×10^{-5})	(3.41)	(4.71×10^{-4})	(1.78×10^{-24})
R-II	$[(H_2O)_2]$	2.18×10^{-20}	1.12	1.37	1.53	3.34×10^{-20}
	5.93×10^{15}	(1.67×10^{-20})	(1.93×10^{-2})	(1.37)	(2.6×10^{-2})	(4.42×10^{-22})
R-X	$[HCOOH]$	5.02×10^{-20}	4.23×10^{3}	1.65	6.98×10^{3}	3.50×10^{-16}
	8.9×10^{10}	(4.99×10^{-20})	(1.48×10^{2})	(2.06)	(3.05×10^{2})	(1.52×10^{-17})
R-XI	$[CH_3COOH]$	2.22×10^{-19}	1.13×10^{4}	---	1.13×10^{4}	2.51×10^{-15}
	8.9×10^{10}	(2.37×10^{-19})	(4.71×10^{2})	(1.67)	(7.87×10^{2})	(1.86×10^{-16})
R-XII	$[H_2SO_4]$	1.12×10^{-19}	2.19×10^{4}	0.72	1.58×10^{4}	1.77×10^{-15}
	3.7×10^{8}	(1.19×10^{-19})	(5.97×10^{2})	(1.71)	(1.02×10^{3})	(1.21×10^{-16})
R-XIII	$[HO_2]$	2.94×10^{-21}	5.21×10^{5}	1.39	7.24×10^{5}	2.13×10^{-15}
	1.4×10^{8}	(1.98×10^{-21})	(4.26×10^{1})	(2.84)	(1.21×10^{2})	(2.39×10^{-19})
Altitude = 0 km, Temperature=310 K						
R-I	$[H_2O]$	5.69×10^{-21}	1.65×10^{-3}	3.69	1.22×10^{-2}	6.93×10^{-23}
	1.45×10^{18}	(5.39×10^{-21})	(2.17×10^{-5})	(3.77)	(1.64×10^{-4})	(8.83×10^{-25})
R-II	$[(H_2O)_2]$	3.89×10^{-20}	4.89×10^{-1}	1.40	6.85×10^{-1}	2.67×10^{-20}
	2.59×10^{15}	(2.96×10^{-20})	(7.41×10^{-3})	(1.40)	(1.04×10^{-2})	(3.07×10^{-22})
R-X	$[HCOOH]$	8.49×10^{-20}	2.27×10^{3}	1.69	3.84×10^{3}	3.26×10^{-16}
	8.9×10^{10}	(8.47×10^{-20})	(7.12×10^{1})	(2.06)	(1.47×10^{2})	(1.24×10^{-17})
R-XI	$[CH_3COOH]$	3.92×10^{-19}	6.16×10^{3}	---	6.16×10^{3}	2.41×10^{-15}
	8.9×10^{10}	(4.22×10^{-19})	(2.31×10^{2})	(1.72)	(3.97×10^{2})	(1.68×10^{-16})
R-XII	$[H_2SO_4]$	1.93×10^{-19}	1.21×10^{4}	0.72	8.71×10^{3}	1.68×10^{-15}
	3.7×10^{8}	(2.05×10^{-19})	(2.92×10^{2})	(1.77)	(5.17×10^{2})	(1.06×10^{-16})

R-XIII	[HO_2] 1.4×10^{8}	4.56×10^{-21} (3.04×10^{-21})	3.18×10^{5} (1.92×10^{1})	1.42 (3.05)	4.52×10^{5} (58.56)	2.06×10^{-15} (1.78×10^{-19})

Table S11: The MP2/aug-cc-pVTZ level predicted rates for the H_2O, $(H_2O)_2$, FA, AA, SA and HO_2 radical assisted H_2CO_3 decomposition reactions (**R-I, R-II, R-X, R-XI, R-XII** and **R-XIII**) with respect to the rate evaluated for the water monomer assisted $H_2CO_3 \rightarrow CO_2 + H_2O$ decomposition reaction (R-I) at 320 and 310 K temperatures and at 0 km altitude of the Earth's environment. The values given in the parenthesis correspond to the results predicted at the CCSD(T)/aug-cc-pVTZ level of calculations.

Altitude (Km)	**Temperature (kelvin)**	**(ν_I/ν_I)**	**(ν_I/ν_{II})**	**(ν_I/ν_X)**	**(ν_I/ν_{XI})**	**(ν_I/ν_{XII})**	**(ν_I/ν_{XIII})**
0	320	1.0	1.4	9.3	1.3	4.4×10^{2}	9.7×10^{2}
		(1.0)	(1.6)	(3.1)	(0.3)	(9.4×10^{1})	(1.3×10^{5})
0	310	1.0	1.5	3.5	0.5	1.6×10^{2}	3.4×10^{2}
		(1.0)	(1.6)	(1.2)	(0.09)	(3.3×10^{1})	(5.1×10^{4})

Table S12: The M06-2X/aug-cc-pVTZ level predicted and ZPE corrected electronic energies (ΔE_{corr}) and free energies (ΔG at 298.15K) of the pre-reactive complexes (RC) and transition states (TS) involved in the water monomer, formic acid and acetic acid assisted H_2CO_3 decomposition reactions. The energies (kcal/mol) of pre-reactive complexes and transition states (TS) have been determined with respect to the total energies of the isolated starting reactant monomers (H_2CO_3 + X) involved in bimolecular encounters. The values marked with blue colour are taken from the works of Kumar et al. (Ref-32-33) for a comparison at the same level of theory. The free energy barriers ($\Delta G^{\#}$) for the unimolecular decomposition steps have been shown separately to avoid the confusion from the effective free energy barriers (free energy of TS with respect to total free energies of starting isolated bimolecular reactants) of the H_2CO_3 decomposition reactions.

Catalyst (X)	$H_2CO_3 + X \rightarrow CO_2 + H_2O + X$				$H_2CO_3\cdots X \rightarrow CO_2\cdots H_2O\cdots X$
	RC ($H_2CO_3\cdots X$)		TS		$\Delta G^{\#}$
	ΔE_{corr}	ΔG	ΔE_{corr}	ΔG	
X = H_2O	-7.46 -7.6	0.89 0.6	14.02 14.5	23.51 23.9	22.62
X = HCOOH	-10.89 -10.8	-0.84 -0.5	1.50 1.6	12.69 12.9	13.53
X = CH_3COOH	-11.70 -12.0	-1.19 -1.9	0.43 0.3	11.89 11.3	13.08

Figure S1: The M06-2X/aug-cc-pVTZ level optimized geometries of pre-reactive complexes and transition states (which are the important species for rate calculations in the forward direction) for the water (H_2O) monomer, formic acid (FA) and acetic acid (AA) assisted carbonic acid (H_2CO_3) decomposition reactions. The geometrical parameters indicated by blue colour are taken from the work of Kumar et al. (Ref-32-33) for a comparison at the same level of theory.

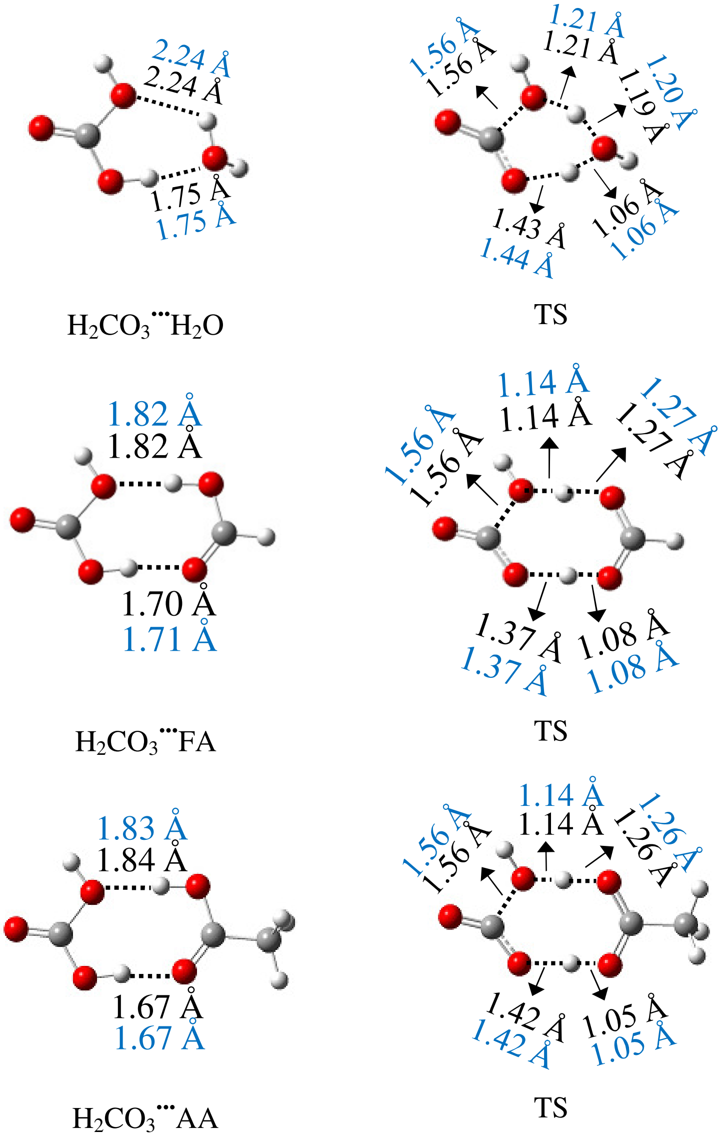

$H_2CO_3{\cdots}H_2O$ TS

$H_2CO_3{\cdots}FA$ TS

$H_2CO_3{\cdots}AA$ TS

Table S13: M06-2X/aug-cc-pVTZ level calculated reaction rates (ν) for both the H_2O and formic acid (HCOOH) assisted H_2CO_3 decomposition reactions at 298.15 K in the unit of sec^{-1}. The values of the equilibrium constants (K_{eq}) for the formation of pre-reactive complexes and rate constants (k_2) of the unimolecular decomposition steps have been given respectively in the unit of cm^3/molecule and sec^{-1}. In table, the Γ represent the tunnelling corrections for the respective reactions and the predicted relative rate is based upon the concentrations (molecule/cm^3) of water and FA those have been reported by Kumar et al. (Ref-32). The values in parenthesis indicated by blue colour have also been shown as reported by Kumar et al. in their correction paper (Ref-33).

$H_2CO_3 + X \rightleftharpoons H_2CO_3\cdots X \rightarrow CO_2\cdots H_2O\cdots X \rightleftharpoons CO_2 + H_2O + X$				
Concentrations	Γ	K_{eq}	k_2	$\nu = K_{eq} * k_2 * \Gamma * [H_2CO_3] * [X]$
$X = H_2O$				
$[H_2O] = 6.1\times10^{17}$	3.80 (3.8)	9.24×10^{-21}	1.59×10^{-4}	$3.41\times10^{-6} \times [H_2CO_3]$ $(0.80\times10^{-6} \times [H_2CO_3])$
X = HCOOH				
$[HCOOH] = 5.0\times10^{10}$	1.47	1.69×10^{-19}	7.42×10^{2}	$9.22\times10^{-6} \times [H_2CO_3]$ $(8.00\times10^{-6} \times [H_2CO_3])$
Relative Rate (ν_{HCOOH}/ν_{H_2O})				
2.7 (10.0)				

As mentioned above, we have calculated the values of K_{eq} and k_2 according to the equation 4 and 5 (see above). It is to be noted here that the resultant value of the (K_{eq} x k_2) can also be calculated directly if we multiply the equation 4 and 5 and use resultant equation[32] that does not involve the energy and partition function of the pre-reactive complex. In addition, for further verification of our data, one can use following three equations[8] as given below to calculate the values equilibrium constants ($K_{eq} \equiv K_c$) and unimolecular decomposition rate constants (k_2) according the free energy values of the pre-reactive complexes and transition states, as given in the Table S12.

$$K_p = \exp\left(\frac{-\Delta G_f}{RT}\right) \qquad (9)$$

$$K_{eq} = K_c = K_p * (RT)^{-\Delta n} \qquad (10)$$

$$k_2 = \left(\frac{k_b T}{h}\right) * \exp\left(\frac{-\Delta G^{\#}}{RT}\right) \qquad (11)$$

In the above equations, ΔG_f and $\Delta G^{\#}$ are respectively the free energy change of the pre-reactive complex when it is formed from the isolated starting bimolecular reactants and free energy barrier for the unimolecular decomposition step in the unit of kcal/mol. Like before, the k_b, h and R are respectively the Boltzmann constant, Planck's constant and universal gas constant. The unit of K_p

and K_c are respectively $(\text{atm})^{-1}$ and (cm^3/molecule), and Δn is the change in number of moles when a pre-reactive complex is formed from the bimolecular isolated starting reactants.

References:

1 C. Eckart, *Phys. Rev.,* 1930, **35**, 1303-1309.

2 R. L. Brown, *J. Res. Natl. Bur. Stand., (U.S.)* 1981, **86**, 357-359.

3 H. S. Johnston and J. Heicklen, *J. Phys. Chem.,* 1962, **66**, 532-533.

4 L. Arnaut, S. Formosinho and H. Burrows, *Chemical Kinetics from Molecular Structure to Chemical Reactivity*, Elsevier, Netherlands, 2007.

5 H. Eyring, *J. Chem. Phys.,* 1935, **3**, 107-115.

6 M. G. Evans and M. Polanyi, *Trans. Faraday Soc.,* 1935, **31**, 875-894.

7 D. G. Truhlar, W. L. Hase and J. T. Hynes, *J. Phys. Chem.,* 1983, **87**, 2664-2682.

8 D. A. McQuarrie, *Statistical Thermodynamics*, Harper and Row, New York, 1973.

9 A. Fernández-Ramos, B. A. Ellingson, R. Meana-Pañeda, J. M. C. Marques and D. G. Truhlar, *Theor. Chem. Acc.,* 2007 **118**, 813-826.

10 J. S. Francisco, M. Torrent-Sucarrat and J. M. Anglada, *J. Am. Chem. Soc.,* 2012, **134**, 20632-20644.

11 J. M. Anglada, G. J. Hoffman, L. V. Slipchenko, M. M.Costa, M. F. Ruiz-López and J. S. Francisco, *J. Phys. Chem. A,* 2013, **117**, 10381-10396.

12 G. J. Frost and V. Vaida, *J. Geophys. Res.,* 1995, **100***,* 18803-18809.

13 A. Razavi, F. Karagulian, L. Clarisse, D. Hurtmans, P. F. Coheur, C. Clerbaux, J. F. Müller and T. Stavrakou, *Atmos. Chem. Phys*., 2011, **11**, 857-872.

14 M. W. Shephard, A. Goldman, S. A. Clough and E. J. Mlawer, *J. Quant. Spectrosc. Radiat. Transfer*., 2003, **82**, 383-390.

15 J. E. Lawrence and P. Koutrakls, *Environ. Sci. Technol*., 1994, **28**, 957-964.

16 S. R. Souza and L. R. F. Carvalho, *J. Braz. Chem. Soc*., 2001, **12**, 755-762.

17 M. Grutter, N. Glatthor, G. P. Stiller, H. Fischer, U. Grabowski, M. Höpfner, S. Kellmann, A. Linden and T. von Clarmann, *J. Geophys. Res., [Atmospheres]* 2010, **115**, D10303.

18 G. Gonz´alez Abad, P. F. Bernath, C. D. Boone, S. D. McLeod, G. L. Manney and G. C. Toon, *Atmos. Chem. Phys*., 2009, **9**, 8039-8047.

19 S. R. Souza, P. C. Vasconcellos and L. R. F. Carvalho, *Atmos. Environ.,* 1999, **33**, 2563-2574.

20 R. W. Talbot, J. E. Dibb, B. L. Lefer, E. M. Scheuer J. D. Bradshew, S. T. Sandholm, S. Smyth, D. R. Blake, N. J. Blake, G. W. Sachse, J. E. Collins and G. L. Gregory, *J. Geophys. Res.,* 1997, **102**, 28303-28313.

21 E. Sanhueja, L. Figueroa and M. Santana, *Atmos. Environ.,* 1996, **30**, 1861-1873.

22 A. Chebbi and P. Carlier, *Atmos. Environ.,* 1996, **30**, 4233-4249.

23 P. Khare, G. S. Satsangi, N. Kumar, K. M. Kumari and S. S. Srivastav, *Atmos. Environ.,* 1997, **31**, 3867-3875.

24 K. Granby and C. S. Christensen, *Atmos. Environ.,* 1997, **31**, 1403-1415.

25 T. Reiner, O. Möhler and F. Arnold, *J. Geophys. Res.,* 1999, **104**, 13943-13952.

26 M. O. Andreae, R. W. Talbot, T. W. Andreae and R. C. Harriss, *J. Geophys. Res.,* 1988, **93**, 1616-1624.

27 R. P. Turco, P. Hamill, O. B. Toon, R. C. Whitten and C. S. Kiang, *J. Atmos. Sci.,* 1979, **36**, 699-717.

28 J. Mao, D. J. Jacob, M. J. Evans, J. R. Olson, X. Ren, W. H. Brune, J. M. S. Clair, J. D. Crounse and K. M. Spencer. M. R. Beaver, P. O. Wennberg, M. J. Cubison, J. L. Jimenez, A. Fried, P. Weibring, J. G. Walega, S. R. Hall, A. J. Weinheimer, R. C. Cohen, G. Chen, J. H. Crawford, C. McNaughton, A. D. Clarke, L. Jaegle, J. A. Fisher, R. M. Yantosca, P. Le Sager and C. Carouge, *Atmos. Chem. Phys*., 2010, **10**, 5823-5838.

29 D. Kubistin, H. Harder, M. Martinez, M. Rudolf, R. Sander, H. Bozem, G. Eerdekens, H. Fischer, C. Gurk and T. Klüpfel. R. Königstedt, U. Parchatka, C. L. Schiller, A. Stickler, D. Taraborrelli, J. Williams and J. Lelieveld, *Atmos. Chem. Phys*., 2010, **10**, 9705-9728.

30 G. P. Brasseur and S. Solomon, *Aeronomy of the Middle Atmosphere*, Springer, Netherlands, 2005.

31 W. B. DeMore, S. P. Sander, D. M. Golden, R. F. Hampson, M. J. Kurylo, C. J. Howard, A. R. Ravishankara, C. E. Kolb and M. J. Molina, Chemical Kinetics and Photochemical Data for Use in Stratospheric Modeling, JPL Publication 97-4, Jet Propulsion Laboratory, California Institute of Technology, Pasadena, CA, 1997.

32 M. Kumar, D. H. Busch, B. Subramaniam and W. H. Thompson, *J. Phys. Chem. A,* 2014, **118**, 5020-5028.

33 M. Kumar, D. H. Busch, B. Subramaniam and W. H. Thompson, *J. Phys. Chem. A,* 2014, **118**, 10155-10156.

34 F. L. Eisele and D. J. Tanner, *J. Geophys. Res*., 1993, **98**, 9001-9010.

35 H. Bardouki, H. Berresheim, M. Vrekoussis, J. Sciare, G. Kouvarakis, K. Oikonomou, J. Schneider and N. Mihalopoulos, *Atmos. Chem. Phys*., 2003, **3**, 1871-1886.

36 J. C. Ianni and A. R. Bandy, *J. Mol. Struct*., *[Theochem]* 2000, **497**, 19-37.

37 J. Zhao, J. N. Smith, F. L. Eisele, M. Chen, C. Kuang and P. H. McMurry, *Atmos. Chem. Phys*., 2011, **11**, 10823-10836.

38 S. Mikkonen, S. Romakkaniemi, J. N. Smith, H. Korhonen, T. Petäjä, C. Plass-Duelmer, M. Boy, P. H. McMurry, K. E. J. Lehtinen, J. Joutsensaari, A. Hamed, R. L. Mauldin III, W. Birmili, G. Spindler, F. Arnold, M. Kulmala and A. Laaksonen, *Atmos. Chem. Phys*., 2011, **11**, 11319-11334.

39 M. Sipila, T. Berndt, T, Petäjä, D. Brus, J. Vanhanen, F. Stratmann, J. Patokoski, R. L. Mauldin III, A. P. Hyvärinen, H. Lihavainen and M. Kulmala, 2010, *Science*, **327**, 1243-1246.

40 B. Temelso, T. E. Morrell, R. M. Shields, M. A. Allodi, E. K. Wood, K. N. Kirschner, T. C. Castonguay, K. A. Archer and G. C. Shields, *J. Phys. Chem. A*., 2012, **116**, 2209-2224.